Korean J. Chem. Eng., 36(8), 1291-1297 (2019)
DOI: 10.1007/s11814-019-0325-8

pISSN: 0256-1115
eISSN: 1975-7220

NH_3-induced removal of NO_x from a flue gas stream by silent discharge ozone generation in a double reactor system

Yujin Hwang*,‡, Abid Farooq*,‡, Sung Hoon Park,‡, Ki Hoon Kim*, Myong-Hwa Lee***, Seuk Cheun Choi****, Min Young Kim**, Rae-su Park*****, and Young-Kwon Park*,†**

*School of Environmental Engineering, University of Seoul, Seoul 02504, Korea
**Department of Environmental Engineering, Sunchon National University, Suncheon 57922, Korea
***Department of Environmental Engineering, Kangwon National University, Chuncheon 24341, Korea
****Thermochemical Energy System R&D Group, Korea Institute of Industrial Technology, Cheonan 31056, Korea
*****Department of Bioenvironmental & Chemical Engineering, Chosun College of Science & Technology, Gwangju 501-744, Korea
(*Received 11 April 2019 • accepted 12 June 2019*)

Abstract−NO_x, a generic term for the nitrogen oxides generated from combustion in the presence of nitrogen, is a serious threat to human health. This study examined the removal of NO_x using ammonia (NH_3) and ozone produced using a silent discharge method. The effects of temperature and residence time on NO_x removal with NH_3 injection in a double reactor system were investigated. An increase in temperature resulted in higher levels of O_3 decomposition, whereas the maximum particle formation in the form of ammonium nitrate (NH_4NO_3) was achieved when both reactors were kept at 180 °C. NH_3 and O_3 injection in large quantities and NO in smaller amounts with a residence time of 10.2 s resulted in the maximum particulate formation. In contrast, when an excess of NH_3 was supplied, it resulted in N_2O formation due to the formation of NH_2 radicals generated from a reaction of NO_2 with NH_3. In addition, 100% NO removal was achieved regardless of the residence time. Kinetic simulations indicated the possibility of moisture being the limiting reactant.

Keywords: Ozone, NO_x Removal, Flue Gas, Ammonium Nitrate, Ammonia

INTRODUCTION

With the increasing demand for, and consumption of, fossil fuels, nitrogen oxides (NO_x) from stationary flue gas emissions pose a serious threat to human health, the ecosystem and the atmosphere [1,2]. Approximately 90% of the total NO_x emission from stationary sources is from vehicle exhaust and other stationary combustion sources (industries) [3]. NO_x is the major pollutant responsible for the generation of acid rain/acid mist and triggers photochemical reactions when combined with hydrocarbons, resulting in the generation of haze and smog. Therefore, it is important to develop NO_x removal technology to remediate environmental pollution.

Several NO_x emission control technologies have been developed to counter this problem, including NO_x storage reduction systems for lean burn engines [4], selective catalytic reduction (SCR) for large scale combustion facilities [5], and three-way catalysts for gasoline fueled vehicles [6]. Among all the NO_x reduction technologies, the conversion of NO to N_2 and O_2 appears to be the most desirable process, but the high temperature requirements and presence of O_2 inhibiting conversion are major difficulties [7]. Pulsed corona or E-beam has attracted recent attention as a denitrification process. Non-thermal plasma is regarded as one of the most viable processes among the potential technologies [8].

Several studies have examined the non-thermal plasma process for denitrification (removal of NO_x) from flue gases and stationary combustion sources, such as diesel power generators, incinerators, and boilers [9-12]. Tsukamoto et al. [13] examined NO_x and SO_2 removal at a thermal power plant using pulsed power (non-thermal plasma) and reported that 90% of NO and SO_2 was removed from the flue gases at the repetition rate of seven pulses/sec and a flow rate of 0.8 *l*/min. Lin et al. [14] examined NO_x removal by plasma-assisted radical injection and NaOH scrubbing. The results revealed a de-NO_x efficiency of 81.2%. Mizuno et al. [15] examined the NO_x removal process using non equilibrium pulse discharged plasma in a simulated flue gas. NO_x reduction from 800 ppm to 300 ppm was observed as a result. Chae [16] reported the mechanism of the use of non-thermal plasma for the treatment of flue gases coming out of diesel exhaust. He deduced that the use of non-thermal induced plasma is a key process for the oxidation of NO to NO_2 and the catalyst system with plasma can achieve high conversion at low temperatures. Furthermore, high particulate removal was observed in the case of plasma.

Many studies have applied hybrid technology to remove NO_x from flue gas streams [17-21]. Yamamoto et al. [17] investigated the removal of NO_x and SO_x simultaneously from flue gas coming out of a glass melting furnace by a semi-dry chemical process and ozone injection combined. They observed the effective oxidation

†To whom correspondence should be addressed.
E-mail: catalica@uos.ac.kr
‡Co-first authors

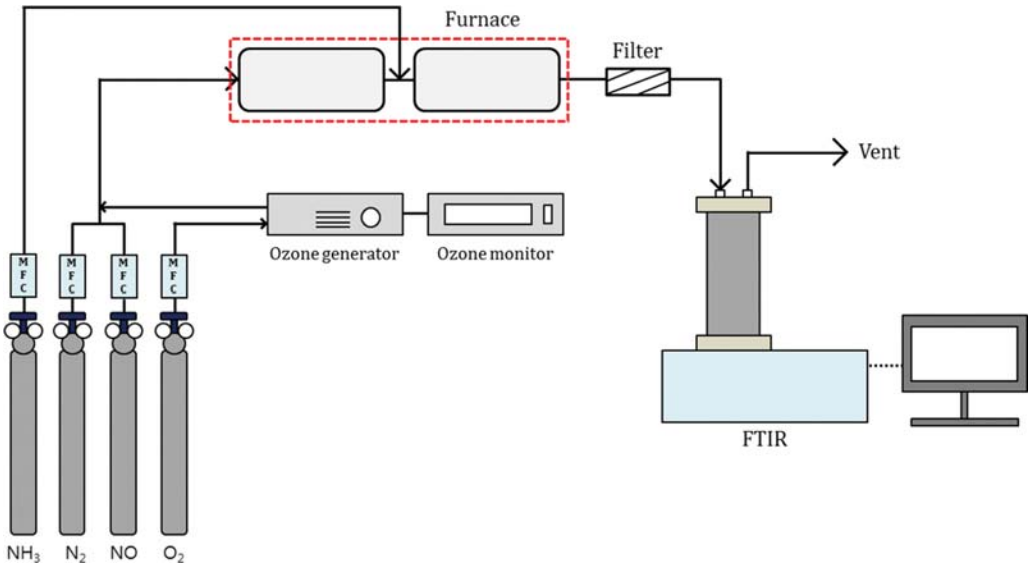

Fig. 1. Schematics of experimental setup.

of NO to NO_2 with the injection of O_3 in the spray region, whereas the removal efficiency of NO and NO_2 was 90% and 50%, respectively. In addition, they achieved 84% removal efficiency for SO_2. Onda et al. [20] performed numerical analysis on the removal of NO_x using an ammonia-assisted pulsed-discharge. They determined that the removal efficiencies for NO increase with increasing electric energy consumption rate in the case of ammonia injection. In contrast, the NO_x removal efficiency declined when excess ammonia was supplied because of the formation of N_2O, a relatively stable compound. Cha et al. [22] examined NO_x removal from 300 hp marine diesel engine exhaust by combining two techniques: selective catalytic reduction using ammonia and the removal of NO_x using non-thermal plasma in a low temperature range of 100-200 °C. They observed a four-fold increase from 20% to 80% in the de-NO_x efficiency at 100 °C compared to SCR alone. In addition, a more than 45% decrease in particulate matter (PM) and a significant alteration in the size distribution of PM after the plasma process were detected.

This study investigated the effects of ammonia injection with respect to temperature and residence time on the removal of NO_x using silent discharge ozone generation in a double reactor system from a flue gas stream. Two reactors were placed in a series where the NO and O_3 reaction was carried out in the first reactor, and the second reactor was for NO_2 conversion to a solid form. Ammonia was injected between the two reactors to achieve the maximum conversion of NO_x. The effects of temperature and residence time on NO conversion were investigated. FTIR spectroscopy was performed to analyze the products after the completion of the reaction. Moreover, the effects of these parameters on particle formation were discussed.

EXPERIMENTAL

The materials used for the process were N_2, O_2, NO, and NH_3 contained in cylinders, whereas ozone (O_3) was generated by an ozone generator and the quantity produced was monitored using an ozone monitor. Fig. 1 presents a schematic diagram of the experimental setup which consisted of four cylinders containing NH_3, N_2, NO, and O_2 along with an ozone generator (OWONE TECH, Ozone generator, LAB-ll) and an ozone monitor. The ozone was generated using a silent discharge method. The cylinders were connected to the reactors with stainless steel connecting the lines. The system consisted of two cylindrical reactors, with 30 cm in length and 6 cm in diameter. The ammonia line was connected between the two reactors. The flow rates of all the gases were controlled using mass flow meters. The reactors were followed by a filter and Fourier transform infrared refractometer (FTIR) to observe the functional groups in the product gas. Overall, the system is very sophisticated for the removal of NO_x from a flue gas stream on the laboratory scale.

As for the methodology, both the reactors were purged with nitrogen for 60 minutes before the start of experiment. After purging, the temperature of the reactors was raised to the required value. The temperature was measured with a thermocouple attached to each reactor. After reaching the required temperature, the O_3 was generated in the ozone generator (OWONE TECH, Ozone generator, LAB-II) using a silent discharge method and was injected along with other feed gases (NO and N_2) into the first reactor, whereas NH_3 was injected into the second reactor. The residence time was controlled by the change in the flow rate of nitrogen, and the reaction was allowed to continue for 6 hr for the generation of solid particles. During the reaction, the product gases were allowed to pass directly to the FTIR attached to the outlet for functional group analysis. The reactors were purged again for 60 min after the completion of reaction to decrease the temperature inside the reactor, and both the reactors were dis-assembled for the collection of solid particles and weight measurement.

REACTION MECHANISM AND KINETIC SIMULATIONS

The ozone generation can be explained by the following mech-

Table 1. Reaction rate constants of the reactions considered

Reaction number	Reaction equation	Reaction rate constant (cm^3/molecules/s*)	Reaction rate constant at 180 °C
	Furnace 01		
R05	$NO+O_3 \rightarrow NO_2+O_2$	1.4E-12exp(−1310/T)	7.774×10^{-14}
R06	$NO_2+O_3 \rightarrow NO_3+O_2$	1.4E-13exp(−2470/T)	6.010×10^{-16}
R07	$NO_3 \rightarrow NO+O_2$	-	
R08	$NO_2+NO_3 \rightarrow N_2O_5$	k_0=3.6E-30(T/300)$^{-4.1}$[N2] k_∞=1.9E-12(T/300)$^{0.2}$ F_C=0.35	4.244×10^{-13}
R09	$2NO_2+H_2O \rightarrow HNO_2+HNO_3$	$3.61\times10^{-17}T^{1.489}\exp(-2121/T)$	3.019×10^{-15}
R10	$H_2O+N_2O_5 \rightarrow 2HNO_3$	$9.51\times10^{-17}(T/298\ K)^{3.354}\exp(-7900\ K/T)$	1.041×10^{-23}
R11	$2HNO_2 \rightarrow NO+NO_2+H_2O$	$1.32\times10^{-24}T^{3.36}\exp(-6764/T)$	3.656×10^{-22}
	Furnace 02		
R13	$HNO_3+NH_3 \rightarrow NH_4NO_3$	1.05E-7	1.050×10^{-7}
R14	$NH_4NO_3 \rightarrow N_2O+2H_2O$	$8.1\times10^{16}T^{-1.44}\exp(-135/T)$	

*Except R9 whose rate constant has the unit of cm^6/molecules^2/s

anism [23]:

$$O_2+e^- \rightarrow O+O+e^-, \quad (1)$$

$$O_2+e^- \rightarrow O_2^+, \quad (2)$$

$$O+O_2+M \rightarrow O_3+M, \quad (3)$$

$$O_2+O_2 \rightarrow O_3+O \quad (4)$$

The reaction mechanism for determining the kinetics of the process can be explained using the following reactions [9,24,25]

$$NO+O_3 \rightarrow NO_2+O_2 \quad (5)$$

$$NO_2+O_3 \rightarrow NO_3+O_2, \quad (6)$$

$$NO_3 \rightarrow NO+O_2, \quad (7)$$

$$NO_2+NO_3 \rightarrow N_2O_5, \quad (8)$$

$$2NO_2+H_2O \rightarrow HNO_2+HNO_3, \quad (9)$$

$$H_2O+N_2O_5 \rightarrow 2HNO_3, \quad (10)$$

$$2HNO_2 \rightarrow NO+NO_2+H_2O \quad (11)$$

$$NO_2+OH+N_2 \rightarrow HNO_3+N_2 \quad (12)$$

NH_4NO_3 is formed as a result of a reaction between NH_3 with HNO_3 [26].

$$HNO_3+NH_3 \rightarrow NH_4NO_3. \quad (13)$$

The decomposition of NH_4NO_3 results in the formation of N_2O and H_2O [27],

$$NH_4NO_3 \rightarrow N_2O+2H_2O. \quad (14)$$

When a suitable amount of NH_3 is available, the removal of NO_2 is achieved with the formation of solid NH_4NO_3. In contrast, if ammonia is supplied in an excess of NO_2, N_2O [20,25], a greenhouse gas, is formed with the release of a large amount of NH_2 as a result of the pulse discharge.

$$H_2O+O \rightarrow 2OH \quad (15)$$

$$NH_3+OH \rightarrow H_2O+NH_2 \quad (16)$$

$$NH_2+NO \rightarrow H_2O+N_2 \quad (17)$$

$$NH_2+NO_2 \rightarrow N_2O+H_2O \quad (18)$$

Kinetic simulations were carried out based on the above-mentioned reaction mechanism to interpret the experimental results. The reaction mechanism given here is a stiff system because many reactions need to be considered and the reaction rates are quite diverse. Therefore, the reactions, whose reaction rates are relatively high, were selected. In addition, the reactions involving electron, oxygen atom, and OH radical were excluded because their concentrations could not be measured. Table 1 lists the reactions and corresponding reaction rate constants available in the literature.

Table 1 shows that R09 and R13 would have much higher reaction rates than other reactions. Therefore, it is expected that the formation of NH_4NO_3 is led mostly by R05, R09, and R13. Furnace 01 was simulated using R05 and R09, whereas Furnace 02 was simulated using R13 only. The fifth-order Runge-Kutta method was used for numerical integration.

RESULTS AND DISCUSSION

1. Effects of Temperature

Fig. 2 shows the effect of the reactor temperature on O_3 decomposition and corresponding FTIR spectra. An increasing trend in O_3 decomposition (Fig. 2(a)) was observed with increasing temperature. The effect has been translated to FTIR spectra, as shown in Fig. 2(b); the lowest peak in terms of absorbance corresponds to the highest temperature (200 °C), whereas the highest can be seen corresponding to the lowest temperature (120 °C).

Fig. 3 presents the effects of temperature on particle formation, while Fig. 4 shows the effects of temperature on O_3 and NH_3 consumption. Three combinations (180 °C-150 °C, 180 °C-180 °C, and

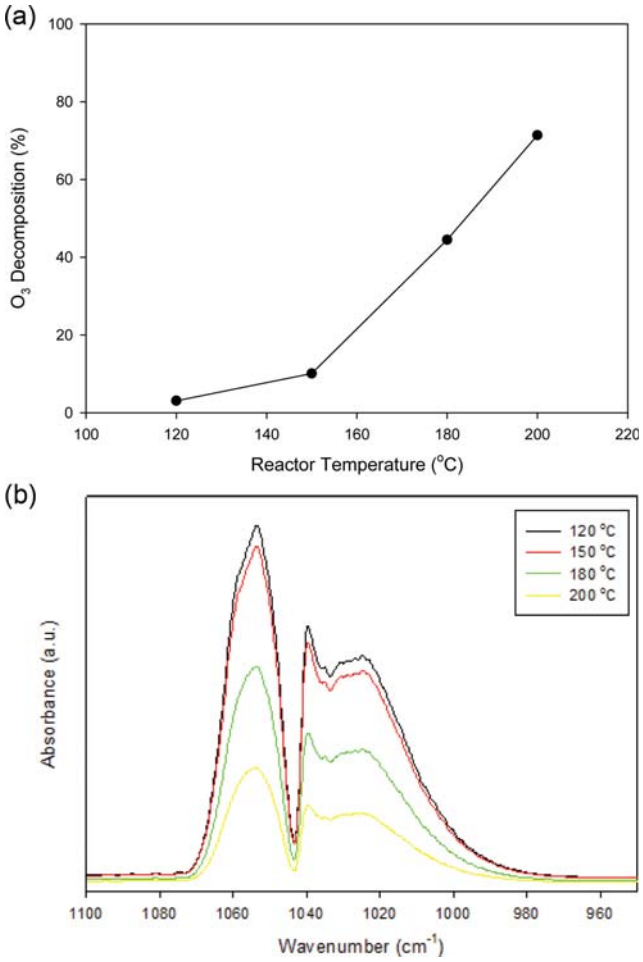

Fig. 2. (a) Effect of Temperature on O_3 decomposition, (b) FTIR at different temperatures.

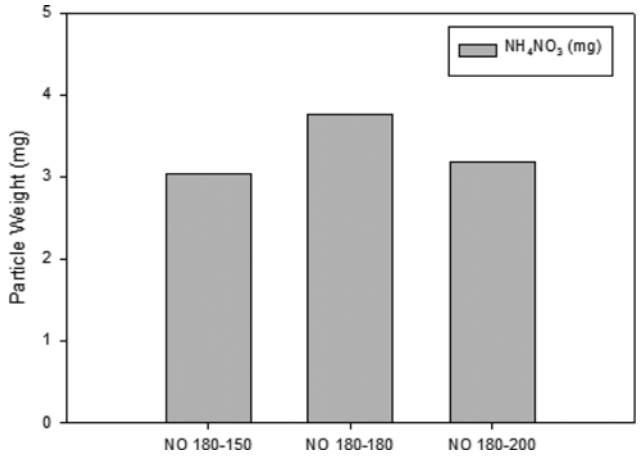

Fig. 3. Effect of temperature on NH_4NO_3 formation.

180 °C-200 °C) for the temperatures of the first and second reactors were investigated to determine the optimal particle formation conditions with an NO and NH_3 concentration of 35 ppm and 66 ppm, respectively. The maximum particle formation was observed when the temperature for both reactors was kept at 180 °C. Therefore, 180 °C was considered the optimal temperature because it gives the maximum consumption of NH_3 and optimal O_3 decomposition for the maximum NO removal and NH_4NO_3 formation, as shown in Fig. 3 and Fig. 4. Higher conversion to NH_4NO_3 corresponds to the higher consumption of O_3 for NO to NO_2 conversion and then NO_2 to NH_4NO_3 with a higher consumption of ammonia. The process can be further explained by the following reaction [20]:

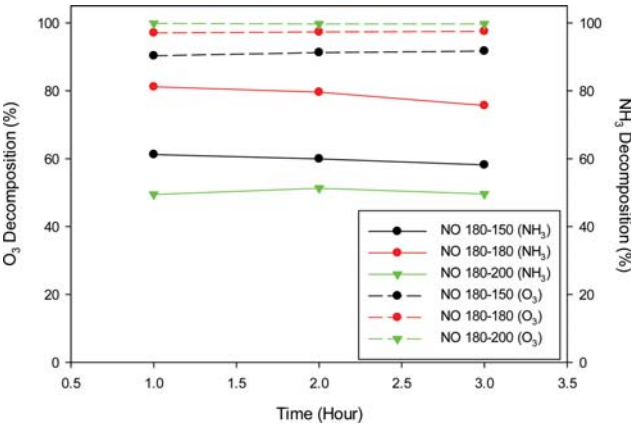

Fig. 4. O_3 and NH_3 consumption rates at different times.

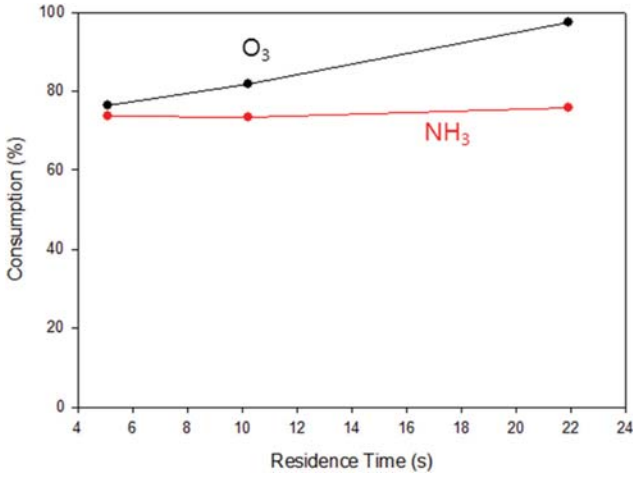

Fig. 5. Effect of residence time on consumption of O_3 and NH_3.

$$NO \xrightarrow{O} NO_2 \xrightarrow{OH} HNO_3 \xrightarrow{NH_3} NH_4NO_3 \quad (19)$$

The NO in the above equation is neutralized with the injection of ammonia, resulting in the conversion of NH_4NO_3. On the other hand, a part of NO_x was also removed and reduced by NH_2 and N radicals formed by NH_3.

2. Effect of Residence Time

Fig. 5 shows the effects of residence time on O_3, NH_3 consumption. The maximum consumption of O_3 and NH_3 was observed at a residence time of 21.9 s and 10.2 s, respectively. Moreover, O_3 consumption increased with increasing residence time but NH_3 remained relatively constant after 10.2 s. Therefore, 10.2 s was considered to be the optimal point in terms of ammonia consumption for the conversion of NO to NO_2. Moreover, the optimal point in terms

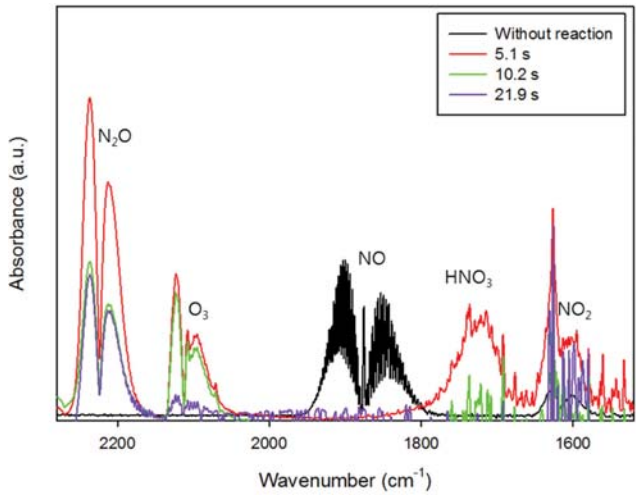

Fig. 6. Effect of residence time on chemical species distribution.

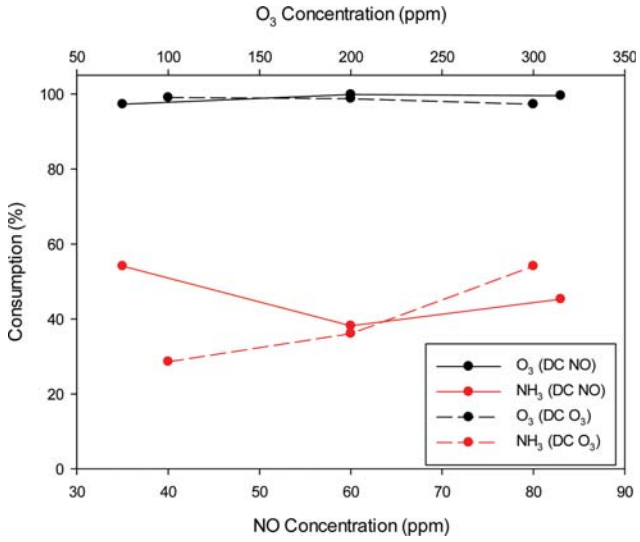

Fig. 7. Effect of injected O_3 and NO concentrations on gas consumption in 10.2 s (DC NO: different concentration of NO, DC O_3: different concentration of O_3).

of residence time could only be decided after particle generation, discussed later in this section. In contrast, NO removal remained at 100%, irrespective of the residence time, as shown in Fig. S1. O_3 and NH_3 consumption is the major factor involved in the conversion of NO_x explained in the next sections.

The IR peaks in Fig. 6 show the effects of residence time on NO consumption and NO_x generation. The peaks represent 100% NO removal, irrespective of the residence time. In contrast, the highest peaks for N_2O and NO_2 were observed at a residence time of 5.1 s. The effect corresponds to the excess of NH_3 [20] in the reactor and insufficient time for the reaction to be completed explained in Eq. (15)-(18). On the other hand, the generation of N_2O and NO_2 was reduced along with less HNO_3 generation, suggesting more production of solid particles in the system. The residence time of 21.9 s resulted in more NO_2 generation with more N_2 injection.

The O_3 concentration plays a vital role in the generation of NO_x.

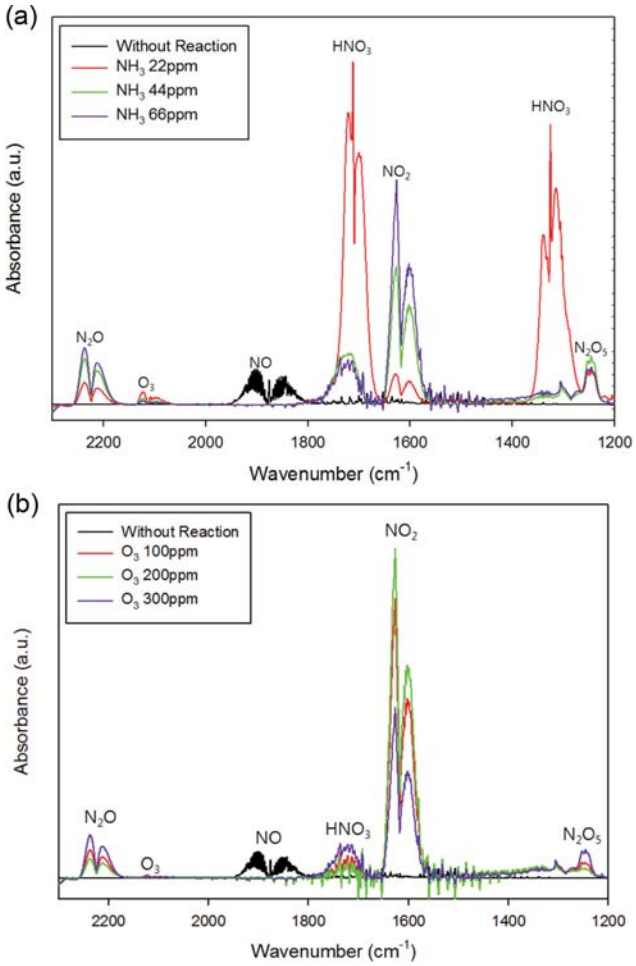

Fig. 8. Effect of injected (a) NH_3 and (b) O_3 concentrations in 10.2 s.

Fig. 7 presents the effects of the O_3 and NO concentration on gas consumption. The maximum NH_3 consumption was observed at 300 ppm of O_3 injection; hence, this was considered to be the optimal O_3 concentration for the process as more NH_3 consumption corresponds to more NH_4NO_3 generation, as explained in Eq. (19). On the other hand, the excess ammonia can result in more N_2O generation due to the formation of a NH_2 radical produced as a result of electron collision [20] when NH_3 reacts with NO_2, as shown in Eqs. (15) and (16). Therefore, it is imperative to perform a stoichiometric calculation before the start of the experiment to inject the required amount of gases. The effect can be observed in Fig. 8(a) and 8(b). The maximum N_2O generation can be seen when 66 ppm and 300 ppm of NH_3 and ozone, respectively, were supplied. Moreover, more NH_3 and O_3 consumption resulted in more particle formation, which is easy to collect, whereas more generation of HNO_3 was observed at low NH_3 concentrations. High NH_3 consumption was observed in the case of 35 ppm of NO, whereas very little change in O_3 consumption was noted throughout the process. Therefore, 35 ppm of NO can be considered the optimal amount to be provided in the process for maximum particle formation (Fig. S2). The lower peaks of NO_2 can be seen with 35 ppm of NO and a higher peak trend was observed with increasing NO concentration.

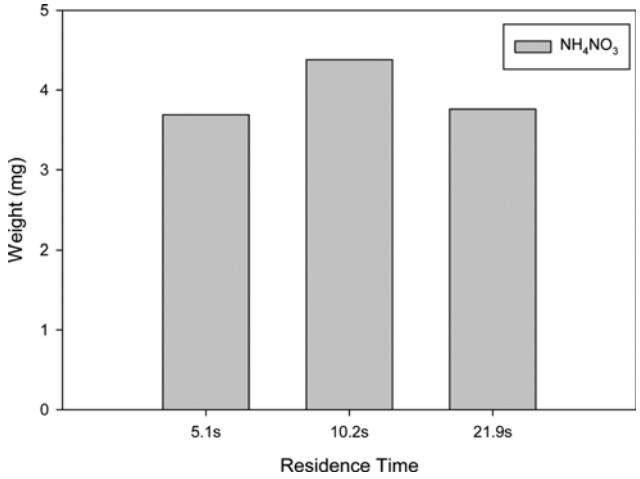

Fig. 9. Effect of residence time on particle formation.

Fig. 9 shows the effects of residence time on particle (NH_4NO_3) formation. The maximum amount of particle formation (4.38 mg) was observed with a residence time of 10.2 s. The effects were due to the larger amount of NH_3 (66 ppm) and O_3 (300 ppm) injection and the lower amount of NO (35 ppm) at the injection point of the second reactor. The higher particle formation was attributed to the NH_3 injection, resulting in the reaction between NH_3 and HNO_3 promoting the oxidation removal process, as shown in Eq. (19). The NH_3, O_3, and NO concentration was chosen based on the IR peaks. The selected concentrations result in the generation of less NO_x and more solid particles (NH_4NO_3), which can be removed easily from the reactor.

3. Kinetic Simulations

Initially, the model was run with excess moisture because there is no information on the moisture content. R05 and R09 ended very quickly (t<0.01 s) owing to the depletion of O_3. The amount of HNO_3 produced was half that of O_3 introduced to the reactor, which is consistent with the stoichiometry of R05 and R09. The amount of NH_4NO_3 produced in Furnace 02 was the same as that of HNO_3 introduced into the furnace.

On the other hand, the amount of NH_4NO_3 collected from Furnace 02 during the experiments was a factor of 10,000 smaller than the model prediction. This suggests that the furnace may have been under oxygen-poor conditions. Therefore, the supply of moisture into the reactor may be a way to promote the conversion of NO to NH_4NO_3. More study will be needed to examine the effects of moisture in the future. Another issue is the effects of oxydizing radicals, such as O and OH, which could not be quantified in this study because of the lack of measurement. This should be another topic of future study.

CONCLUSION

The NH_3-induced removal of NO_x using silent discharge ozone generation with respect to temperature and residence time in a double reactor system was investigated and the following conclusions were made:

- Ozone (O_3) decomposition increased with increasing temperature, while maximum particle formation was obtained with the temperature combination of 180 °C-180 °C. The effect was attributed to the maximum consumption of ammonia in this temperature range.
- The consumption of O_3 increased with increasing residence time, whereas the consumption of NH_3 was relatively constant with increasing residence time.
- NO removal was 100%, irrespective of the residence time.
- The residence time of 10.2 s, NH_3 injection of 66ppm, O_3 injection of 100 ppm, and NO injection of 35 ppm resulted in the maximum particle formation, which is easy to collect and safer for the environment.
- Ammonium nitrate (NH_4NO_3) was formed after NH_3 injection due to the reaction between NH_3 and HNO_3, promoting the oxidation removal process. The process was also promoted by the formation of NH_2 radicals formed due to the electron collision dissociation of NH_3. Both processes improved the NO_x removal performance.
- The formation of N_2O occurred as a result of a NH_2 radical reaction with NO_2 formed due to electron collision with ammonia when an excess of NH_3 and shorter residence time was supplied.
- Kinetic simulations indicated that moisture might have been the limiting reactant for the formation of NH_4NO_3. More study will be needed to quantify the effects of moisture and oxidizing radicals.

ACKNOWLEDGEMENTS

This research was supported by the National Strategic Project-Fine particle of the National Research Foundation of Korea (NRF) funded by the Ministry of Science and ICT (MSIT), the Ministry of Environment (ME), and the Ministry of Health and Welfare (MOHW) (2017M3D8A1092029).

SUPPORTING INFORMATION

Additional information as noted in the text. This information is available via the Internet at http://www.springer.com/chemistry/journal/11814.

REFERENCES

1. Y. Xiong, Y. Zeng, W. Cai, S. Zhang, J. Ding and Q. Zhong, *J. Ind. Eng. Chem.*, **65**, 380 (2018).
2. X. Long, B. Duan, H. Cao, M. Jia and L. Wu, *J. Ind .Eng. Chem.*, **62**, 217 (2018).
3. H. Wang, X. Li, P. Chen, M. Chen and X. Zheng, *Chem. Commun.*, **49**, 9353 (2013).
4. S. Roy and A. Baiker, *Chem. Rev.*, **109**, 4054 (2009).
5. Y. Fan, W. Ling, B. Huang, L. Dong, C. Yu and H. Xi, *J. Ind. Eng. Chem.*, **56**, 108 (2017).
6. M. Shelef and R. W. McCabe, *Catal. Today*, **62**, 35 (2000).
7. F. Garin, *Appl. Catal. A: Gen.*, **222**, 183 (2001).
8. S. Tsukamoto and T. Namihira, Pulsed Power Conference, Monterey, CA, 1330 (1999).
9. J. O. Chae, *J. Electrostatics*, **57**, 251 (2003).
10. J. O. Jo and Y. S. Mok, *Appl. Chem. Eng.*, **29**, 92 (2018).

11. H. Fujishima, K. Takekoshi, T. Kuroki, A. Tanaka, K. Otsuka and M. Okubo, *Appl. Energy*, **111**, 394 (2013).
12. T. Kuroki, M. Takahashi, M. Okubo and T. Yamamoto, *IEEE Trans. Ind. Appl.*, **38**, 1204 (2002).
13. S. Tsukamoto, T. Namihira, D. Wang, S. Katsuki, H. Akiyama and E. Nakashima, Digest of Technical Papers 12th IEEE International Pulsed Power Conference (Cat No99CH36358), 2, 1330 (1999).
14. H. Lin, X. Gao, Z. Y. Luo, S. P. Guan, K. F. Cen and Z. Huang, *J. Environ. Sci. (China)*, **16**, 462 (2004).
15. A. Mizuno, R. Shimizu, A. Chakrabarti, L. Dascalescu and S. Furuta, *IEEE Trans. Ind. Appl.*, **31**, 957 (1995).
16. J. O. Chae, *J. Electrostatics*, **57**, 251 (2003).
17. Y. Yamamoto, H. Yamamoto, D. Takada, T. Kuroki, H. Fujishima and M. Okubo, *Ozone: Sci. Eng.*, **38**, 211 (2016).
18. H. W. Park and S. Uhm, *Appl. Chem. Eng.*, **28**, 607 (2017).
19. J. S. Cha, J. W. Park, B. Jeong, H. D. Kim, S. S. Park and M. C. Shin, *Appl. Chem. Eng.*, **28**, 576 (2017).
20. O. Kazuo, K. Hironobu, I. Kohei and H. Ibaraki, *J. Appl. Phys.*, **95**, 3928 (2004).
21. B. Guan, H. Lin, Q. Cheng and Z. Huang, *Ind. Eng. Chem. Res.*, **50**, 5401 (2011).
22. M. S. Cha, Y.-H. Song, J.-O. Lee and S. J. Kim. *Int. J. Plasma Environ. Sci. Technol.*, **1**, 28 (2007).
23. J. Kitayama and M. Kuzumoto, *J. Phys. D: Appl. Phys.*, **30**, 2453 (1997).
24. K. Nishimura and N. Suzuki, *J. Nuclear Sci. Technol.*, **18**, 878 (1981).
25. R. Atkinson, D. L. Baulch, R. A. Cox, J. N. Crowley, R. F. Hampson and R. G. Hynes, *Atmos. Chem. Phys.*, **4**, 1461 (2004).
26. D.-J. Kim, Y. Choi and K.-S. Kim, *Plasma Chem. Plasma Process.*, **21**, 625 (2001).
27. G. Feick and R. M. Hainer, *J. Am. Chem. Soc.*, **76**, 5860 (1954).